Direct displacement-based assessment with nonlinear soil–structure interaction for multi-span reinforced concrete bridges

Pengpeng Ni[a], Lorenza Petrini[b]* and Roberto Paolucci[b]

[a]*ROSE Programme, UME (Understanding and Managing Extremes) Graduate School, IUSS Pavia (Institute for Advanced Study, Pavia), Via Ferrata 1, 27100 Pavia, Italy;* [b]*Department of Civil and Environmental Engineering, Politecnico di Milano, Piazza Leonardo da Vinci 32, 20133 Milano, Italy*

(*Received 23 May 2012; final version received 20 January 2013; accepted 2 May 2013*)

Nomenclature

M_N: nominal moment of the member
M_U: ultimate moment of the member
$M_{F,LIM}$: limit overturning moment of the foundation leading to bearing capacity failure
M_F: moment acting on the foundation determined from base shear
$M_{P-\Delta}$: moment induced by P–Δ effect
Φ_Y: yielding curvature of the member
Φ_U: ultimate curvature of the member
F_Y: yielding force of the member
F_U: ultimate force of the member
Δ_Y: yielding displacement of the member
Δ_U: ultimate displacement of the member
Δ_{SL}: limit state displacement of the member
Δ_S: displacement of the pier top due to structure deformation
Δ_F: displacement of the pier due to foundation rotation
Δ: critical pier total displacement
Δ_{cap}: displacement capacity for equivalent SDOF system of the bridge
Δ_{TOT}: total displacement of the pier
Δ_{A1}, Δ_{A2}: displacement of the abutments
$\Delta_{cap\text{-}el}$: elastic displacement capacity of the bridge
$\Delta_{dem\text{-}el}$: elastic displacement demand of the bridge
H: pier height
L_C: length from the base section to the contraflexure point in the member
V: base shear force of the pier
V_{A1}, V_{A2}: base shear force of the abutments
V_{base}: total base shear force of the bridge
K_F: rotational secant stiffness of the foundation
$K_{F,0}$: initial elastic rotational stiffness of the foundation
K_e: effective stiffness of the global equivalent SDOF system
K_{eq}: equivalent stiffness of the SDOF fixed-base oscillator
ξ_S: superstructure damping ratio
ξ_{A1}, ξ_{A2}: elastic damping ratio of the abutment
ξ_{ss}: elastic damping ratio of the superstructure
ξ_{eq}: damping ratio of the equivalent SDOF fixed-base oscillator
ξ_{sys}: global system damping ratio of the bridge
ξ_F: rotational damping ratio of the foundation
$\xi_{F,0}$: initial elastic rotational damping ratio of the foundation
θ: foundation rotation

*Corresponding author. Email: lorenza.petrini@polimi.it

θ_{LIM}: limit foundation rotation
θ_{Δ}: stability index
N_{max}: vertical static bearing capacity of the foundation
N: total static vertical load applied in the foundation
FS: static safety factor of the foundation
m_e: equivalent mass of the bridge
m_S: superstructure mass
B, L: sides' length for rectangular foundation
R_a: radius for circular foundation
R_{eq}: equivalent radius for rectangular foundation
h_F: constant embedment depth of the foundation
G: shear modulus of the sand
ν: Poisson's ratio of the sand
D_R: relative density of the sand
φ: friction angle of the sand
c: cohesion of the sand
V_s: shear wave velocity of the sand
μ: ductility of the pier
T_e: effective period of the bridge
T_{eq}: vibration period of the equivalent SDOF fixed-base oscillator
R: spectral reduction factor
C/D: safety factor determined by capacity/demand ratio
σ: standard deviation
c_v: coefficient of variation
x_i: capacity/demand ratio for the ith accelerogram
x_m: mean of the capacity/demand ratios

1. Introduction

The integrity and full serviceability of bridges, such as highway viaducts, may be of major relevance after an earthquake as they have a fundamental role in the civil protection emergency response. In Italy, like in other seismic countries, as many of these 'strategic' bridges have been built either before seismic design provisions were enforced or based on old seismic design criteria, the implementation of an efficient and relatively simple seismic assessment procedure could be a useful tool to identify structures at risk and to plan rehabilitation works.

For this purpose, we have based our research on the framework of the direct displacement-based assessment (DDBA) procedure, introduced by Priestley (1997), encouraged by the results obtained in recent investigations (Cardone, Perrone, & Sofia, 2011; Petrini, Şadan, & Calvi, 2009; Şadan, 2009; Şadan, Petrini, & Calvi, 2012) that applied this approach for the study of simplified bridge configurations, including several existing bridges. Other research works (Dwairi & Kowalsky, 2006; Kappos, Gidaris, & Gkatzogias, 2012; Suarez & Kowalsky, 2011) that have been conducted to accurately evaluate the seismic displacement pattern of bridges provide significant confidence to the DDBA approach. The novelty of the work presented herein is the introduction of nonlinear soil–structure interaction (NLSSI) effects – based on Paolucci, Figini, and Petrini's (2013) displacement-based design approach for individual bridge piers – within the DDBA bridge assessment framework established by Şadan et al. (2012).

In contrast to linear soil–structure interaction effects, the role of which on the seismic response of structures has been discussed (see, for example, Kausel, 2010; Mylonakis & Gazetas, 2000; Mylonakis, Syngros, Gazetas, & Tazoh, 2006), research on the contribution of NLSSI effects on the seismic response of structures is still under development. As pointed out in several recent theoretical and experimental contributions, for a summary of which the reader is referred to Pecker, Paolucci, Chatzigogos, Correia, and Figini (2012), nonlinear response of the soil–foundation system is almost unavoidable during moderate-to-strong earthquakes, with potential temporary mobilisation of the bearing capacity of the foundation and development of permanent displacements and rotations. In particular, centrifuge and shaking table experiments on simple soil–foundation–structure systems have shown that NLSSI effects may lead to a substantial reduction in the seismic demand on the structure, with a balanced distribution of energy dissipation between the foundation and the structure (Deng, Kutter, & Kunnath, 2012; Drosos et al. 2012; Liu et al. 2012). Accordingly, the seismic demand on the structure, and the consequent risk assessment, is generally overestimated, although in some cases it could be underestimated, when no adequate considerations on NLSSI effects are integrated in the framework of evaluation methodology.

Referring, in particular, to the introduction of NLSSI into the performance-based design or assessment of bridges, Kwon and Elnashai (2010) pointed out that nonlinear dynamic finite-element simulations including simultaneously the soil–foundation–bridge system are very costly from a computational point of view and not suitable to perform parametric analyses. Ghalibafian, Foschi, and Ventura (2008) proposed a simple estimation of the NLSSI effects on the ductility and displacement demand of bridge piers based on the modification of the fixed-based demand by applying the fraction of the flexible-based period to the fictitious fixed-based period of the piers. Sextos, Kappos, and Pitilakis (2003) and Sextos, Pitilakis, and Kappos (2003) developed a lumped plasticity model for the piers using inelastic springs located at their ends with the dynamic impedance matrices for coupled horizontal and rocking modes of vibration, and applied it to the parametric study of 20 bridges with NLSSI effects.

More recently, Paolucci et al. (2013) proposed a simplified procedure to introduce NLSSI effects on the direct displacement-based design (DDBD) of single bridge piers. The procedure is based on the use of empirical

curves to evaluate the rotational stiffness degradation ($K_F/K_{F,0}$) and the increase of damping ratio ξ_F as a function of foundation rotation (θ). Iterations are performed to ensure that admissible values of foundation rotations are complied, in addition to the standard checks on structural displacements and drifts. In Figure 1, a set of such curves is presented for shallow foundations on dry sands, as a result of a parametric study, illustrated in more detail by Paolucci, di Prisco, Figini, Petrini, and Vecchiotti (2009). Empirical formulas for both $K_F/K_{F,0}(\theta)$ and $\xi_F(\theta)$ as a function of the static safety factor N_{max}/N (where N_{max} is the vertical static bearing capacity and N is the element static vertical load, including the masses of foundation, pier and related part of the deck) are introduced for dense ($D_R = 90\%$) and medium-dense ($D_R = 60\%$) soil conditions. An extended set of such curves is under development, based on the availability of new macro-element model, which is applicable to both cohesive and granular materials and deep foundations (Correia, 2011).

The main idea behind the procedure introduced by Paolucci et al. (2013) is the formulation of a linear equivalent oscillator, following the principles of DDBD, with equivalent period and damping modified according to the nonlinear variability of foundation stiffness and damping with foundation rotation, as illustrated in Figure 1. In this paper, the aforementioned procedure is extended to provide a simplified, yet effective, framework, in which NLSSI effects can be incorporated within the DDBA of straight multi-span single pier reinforced concrete bridges. Following the description of the main steps of the procedure, its application in a set of simplified bridge configurations is presented. The reliability of the procedure is evaluated performing nonlinear time-history analyses, while the influence of NLSSI on the bridge assessment is considered comparing DDBA + -NLSSI and DDBA results. In the concluding section, the limitations and potential applications of the presented methodology are discussed.

2. Direct displacement-based assessment with NLSSI procedure

As aforementioned, the DDBA + NLSSI procedure presented in this paper is an extension of the DDBA developed by Şadan et al. (2012) by including NLSSI effects via an iterative linear-equivalent process developed by Paolucci et al. (2013). Following the original formulation by Şadan et al. (2012), the proposed approach is applicable to simple bridge configurations having

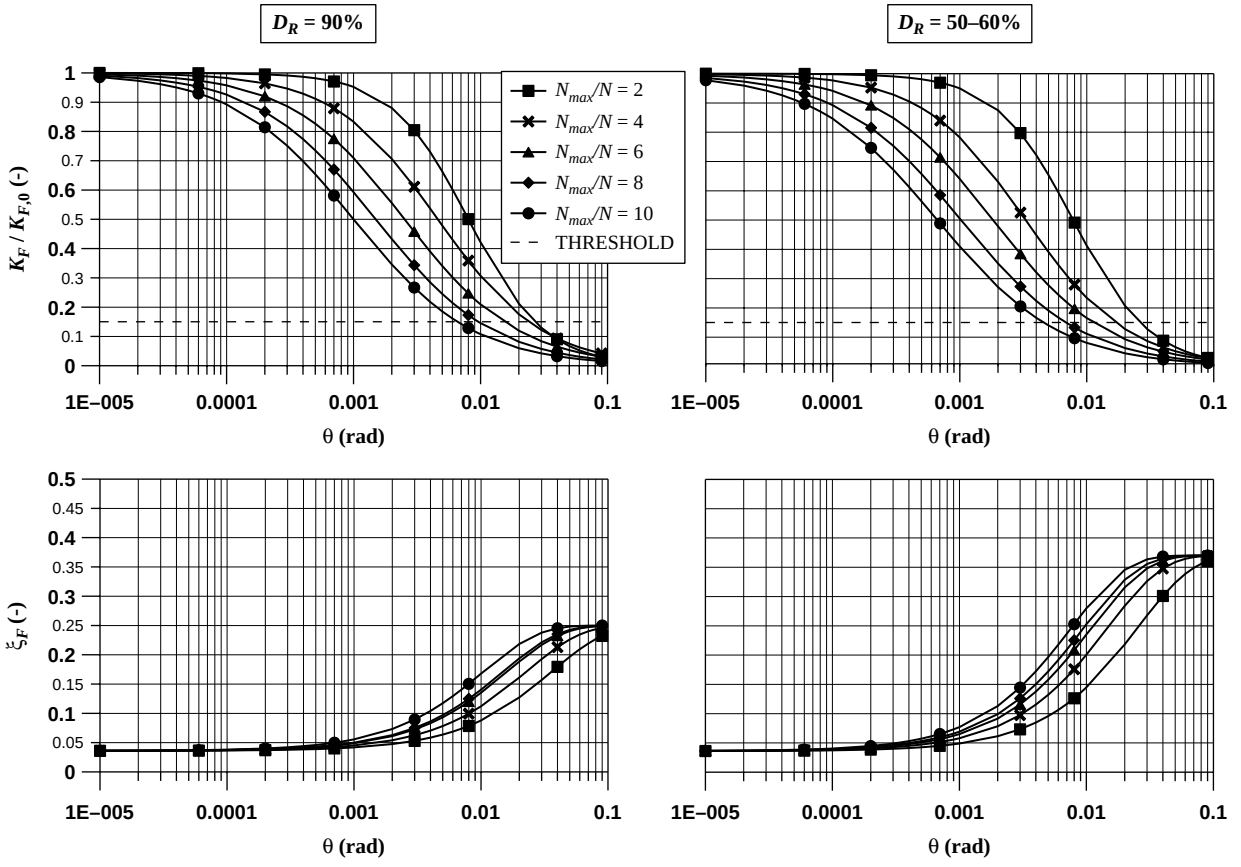

Figure 1. Influence of the loading conditions on the rotational secant stiffness degradation (top) and damping increase (bottom), for dense (left) and medium dense (right) sand. Adapted from Paolucci et al. (2009).

single-column piers and continuous deck supported on bearings, or monolithically connected with the piers without expansion/seismic gaps. Moreover, the failure in the structure is only due to the attainment of maximum displacement capacity of one of the piers, while superstructure and abutments behave elastically and deformation of bearing devices is neglected.

In the following, the DDBA + NLSSI procedure is described highlighting its novelty with respect to DDBA. In the DDBA + NLSSI procedure, three main steps can be recognised: (1) for each pier on flexible foundation, the equivalent Single Degree-of-Freedom (SDOF) system is obtained; then (2) the whole bridge is reduced to an SDOF system; and finally, (3) the assessment of the bridge is performed. These steps are described in detail in the following subsections.

2.1. Step 1: simplification of each pier on flexible foundation as SDOF system

Step 1 (S1) is divided into sub-steps as depicted in Figure 2, which have to be repeated for each pier as described in the following.

S1.1. Determination of the pier characteristics for a given limit state

As common in assessment procedure, all available structural information (material properties, section geometry, reinforcement type and quantity) should be collected by *in situ* inspections or structural drawings and calculations. The final goal is to describe the nonlinear behaviour of each pier of the bridge in an approximate way through a force–displacement curve: it will be used to calculate the shear force value corresponding to a given pier top displacement. Following DDBA (Şadan et al., 2012), using the obtained material properties and associated limit material strain values for the limit state being considered as usually given in seismic codes, moment–curvature analysis for each pier is performed.

The resulting curve is bilinearised, detecting the two points yielding curvature Φ_Y – nominal moment M_N and ultimate curvature Φ_U – ultimate moment M_U, and used to derive the force–displacement relation, characterised by the two points yielding displacement Δ_Y – yielding force F_Y and ultimate displacement Δ_U – ultimate force F_U. The authors refer to Priestley, Calvi, and Kowalsky (2007) for the description of the bilinearisation process, the definition of the yielding, nominal and ultimate points according the pier end-fixity conditions (whether they are connected to the deck monolithically or by means of bearings) and the interaction between pier flexural ductility and shear strength.

In particular, the flexural ductility–shear strength interaction is calculated using the modified University of California, San Diego (UCSD) model (Priestley, Seible, & Calvi, 1996). At the end of this step, for a given limit state, considering the single pier fixed at the base, it is possible to

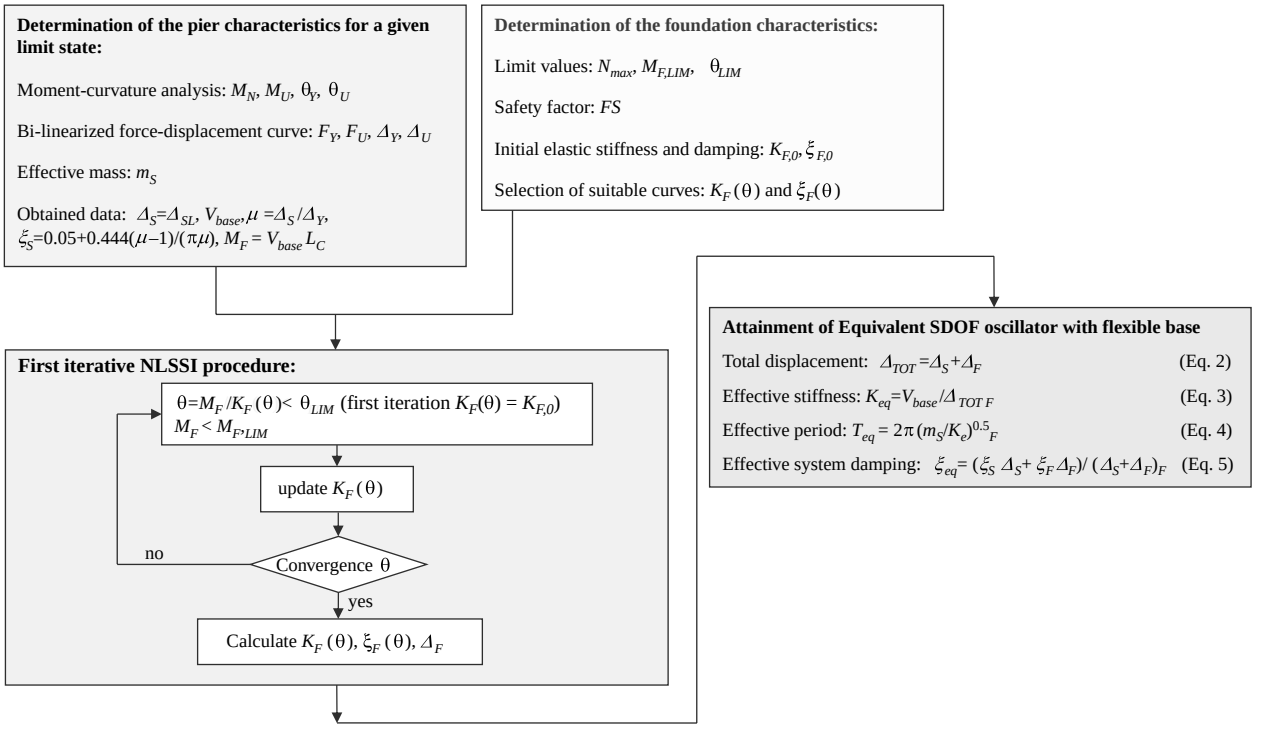

Figure 2. Step 1: simplification of each pier on flexible foundation as SDOF system.

calculate the limit state displacement Δ_{SL} due to the structure deformation. Hence, from the bilinearised curve, the base shear V_{base} is obtained and the base moment transmitted to the foundation is equal to $M_F = V_{base} \cdot L_C$, where L_C is the length from the base section to the contraflexure point in the member (taking into account different end-fixity conditions). The mass of each pier m_S is calculated as the combination of one-third of the overall pier mass and the deck load portion which rests on it (Priestley et al., 1996). Finally, the ductility μ is calculated as the ratio between the maximum displacement reached by the structure; in this step, $\Delta_S = \Delta_{SL}$, and the yielding displacement Δ_Y. If the pier remains in the elastic range, μ is assumed to be equal to one. The damping of the pier is obtained by the sum of an elastic and inelastic contribution (Grant, Blandon, & Priestley, 2005):

$$\xi_S = 0.05 + \frac{0.444(\mu - 1)}{\mu\pi}. \quad (1)$$

S1.2 Determination of the foundation characteristics

For each foundation, all available information in terms of soil properties (shear modulus G, Poisson's ratio ν and relative density D_R), foundation geometry (height H and radius R for circular shape or sides length B and L for rectangular shape) and material characteristics (density) should be collected by *in situ* inspections or structural drawings and calculations. The final goal is to evaluate the following parameters: (i) the vertical static bearing capacity, N_{max}; (ii) the corresponding static safety factor, $FS = N_{max}/N$; (iii) the limit overturning moment $M_{F,LIM}$, leading to bearing capacity failure, and the limit foundation rotation θ_{LIM}; (iv) the initial elastic rotational stiffness $K_{F,0}$ and damping ratio $\xi_{F,0}$, determined by standard formulas (e.g. Gazetas, 1991) reported in Table 1. The equivalent radii can be used to transform a rectangular foundation ($B \times L$) into a circular foundation (R) according to Table 2. At the end of this step, the empirical curves describing the variations in foundation rotational secant stiffness and damping factor are calculated.

Table 1. Initial elastic rotational stiffness of the foundation.

Mode	Strip	Circular
Rotational stiffness	$K_{F,0} = \frac{0.5\,GB^3}{1-\nu}$	$K_{F,0} = \frac{GD^3}{3(1-\nu)}$

S1.3 First iterative procedure for taking NLSSI into account

In this sub-step [not present in the standard DDBA procedure proposed by Şadan et al. (2012)], the NLSSI effects on each single pier, considered separately from the others, are defined. In particular, it is assumed that the displacement of the pier top due to structure deformation Δ_S is equal to the limit displacement Δ_{SL} calculated in the sub-step S1.1. Accordingly, V_{base} and hence M_F, also known from sub-step S1.1, are fixed into this sub-step. The single pier on flexible foundation is simply modelled by a system with two degrees of freedom (2DOF), i.e. the relative displacement of the structure Δ_S and the foundation rotation θ, in which the structure and the foundation are represented by two springs in series (Figure 3, left).

The foundation rotation causes a lateral displacement $\Delta_F = \theta H$ at the top of the oscillator, where H denotes its height. For simplicity, we will neglect foundation flexibility in the horizontal direction, as well as the contribution of the foundation mass to the total mass m_S (Wolf, 1985) of the structure. Once $M_{F,LIM}$, θ_{LIM} and $K_F(\theta)$ are known from the sub-step S1.2 and the condition $M_F < M_{F,LIM}$ has been verified, an iterative process (summarised in Figure 2) is performed calculating the rotation $\theta < \theta_{LIM}$ induced into the foundation by M_F and the corresponding values of $K_F(\theta)$. At the first iteration, K_F is set equal to $K_{F,0}$, thus, the initial value of θ is the rotation on an elastic soil θ_0. The iterative process reaches convergence when there is no significant change in foundation rotation θ between two subsequent iterations. When convergence is reached, the foundation damping $\xi_F(\theta)$ and the rigid displacement induced by the foundation rotation Δ_F are also calculated.

S1.4 Attainment of equivalent SDOF oscillator with flexible base

The maximum displacement the pier can reach for a given limit state is given by

$$\Delta_{TOT} = \Delta_S + \Delta_F = \Delta_{SL} + \Delta_F. \quad (2)$$

Table 2. Equivalent radii of rectangular footings for different degree of freedom.

Degree of freedom	Translation	Rocking		Torsion
		About x-axis	About y-axis	About z-axis
Equivalent radius, R_{eq}	$\left(\frac{BL}{\pi}\right)^{1/2}$	$\left(\frac{BL^3}{3\pi}\right)^{1/4}$	$\left(\frac{B^3L}{3\pi}\right)^{1/4}$	$\left(\frac{BL(B^2+L^2)}{6\pi}\right)^{1/4}$

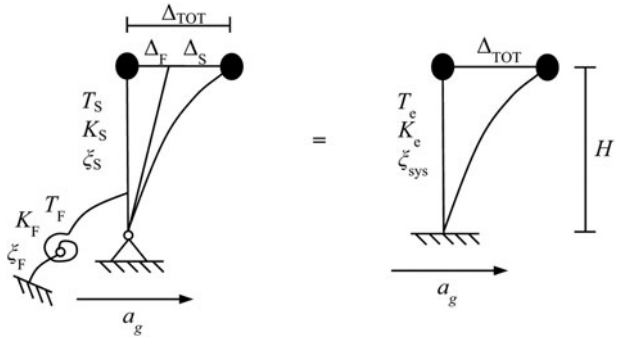

Figure 3. Left: 2DOF system representative of a harmonic oscillator subject to base acceleration and with rotational compliance of the foundation. Right: equivalent SDOF according to Priestley et al. (2007).

Following Priestley et al. (2007), the 2DOF compliant system is replaced by an equivalent SDOF fixed-base oscillator (Figure 3, right) characterised by the equivalent stiffness K_{eq}, vibration period T_{eq} and damping ratio ξ_{eq} defined by Equations (3)–(5):

$$K_{eq} = \frac{V_{base}}{\Delta_{TOT}}, \tag{3}$$

$$T_{eq} = 2\pi\sqrt{\frac{m_S}{K_{eq}}}, \tag{4}$$

$$\xi_{eq} = \frac{\xi_F\Delta_F + \xi_S\Delta_S}{\Delta_F + \Delta_S}. \tag{5}$$

2.2. Step 2: reduction of the bridge to a SDOF system

Once defined the behaviour of each single pier, the interaction among them has to be taken into account for obtaining the definition of the displacement profile of the structure at the given limit state, which depends on the bridge geometry and stiffness ratio between the elements. Owing to the high lateral stiffness provided by the superstructure in the longitudinal direction, together with the simplified assumptions that the deck remains in elastic range, deformation of bearing devices is neglected and no movement joints are considered; during a longitudinal seismic excitation, it can be assumed that all piers have the same displacement. Accordingly, the pier with the lower displacement capacity will limit the maximum displacement of the other piers and hence it will determine the displacement of the whole bridge. This assumption is crucial in order to simplify the process of the first-level screening of existing bridges with potentially important NLSSI effects.

Conversely, in transverse direction, a cumbersome iterative procedure, based on eigenvalue analysis (Dwairi & Kowalsky, 2006; Kowalsky, 2002), called iterative eigenvalue analysis (IEA) has to be used. Hence, in this step (S2), two different paths have to be followed for the longitudinal and transversal directions, as summarised in Figure 4. However, in both cases, a second iterative procedure has to be performed for evaluating the influence of NLSSI effects on the global behaviour of the bridge. Since the focus is given in describing the novelty of DDBA + NLSSI, the introduction of the second iterative procedure in the case of longitudinal seismic action will be briefly described, and only the most significant differences in the case of transversal action will be discussed.

S2.1 Derivation of the bridge displacement shape in longitudinal direction

At the end of step 1, the converged total displacement $\Delta_{TOT,i}$ of each ith pier will be compared and, because of the hypothesis of equal displacement of all the piers, the smallest one will govern the analysis. This pier is regarded as the critical pier, and the corresponding total displacement, denoted as Δ, will restrict the displacement of other piers.

S2.2 Second iterative NLSSI process

The critical pier displacement is the target total displacement for all piers. NLSSI effects play an important role in changing the overall displacement capacity of the pier and foundation system compared with the fixed-base case. In order to find for each pier and related foundation the altered displacement corresponding to the target total displacement, a second iterative NLSSI process has to be performed, as described in the following steps:

(i) Since for each ith pier the total displacement is known ($\Delta_{TOT,i} = \Delta$), the structural displacement $\Delta_{S,i}$ is determined as

$$\Delta_{S,i} = \Delta - \Delta_{F,i} \leq \Delta_{SL,i}. \tag{6}$$

The maximum achievable displacement of each pier is restricted by the limit state displacement $\Delta_{SL,i}$ calculated in step 1, and therefore, as a starting point of the second iterative NLSSI process, the foundation displacement $\Delta_{F,i}$ is assumed to be equal to $\Delta - \Delta_{SL,i}$. If the total target displacement Δ is smaller than ith pier's limit state displacement, the foundation displacement should start from zero.

(ii) The base shear V_i is evaluated from the computed structural displacement $\Delta_{S,i}$ by the bilinear force–displacement curve of the ith pier obtained in step 1. At this stage, however, the stability index of the system $\theta_{\Delta,i}$, given by the ratio between the moment due to P–Δ effect ($M_{P-\Delta,i}$) and overturning moment

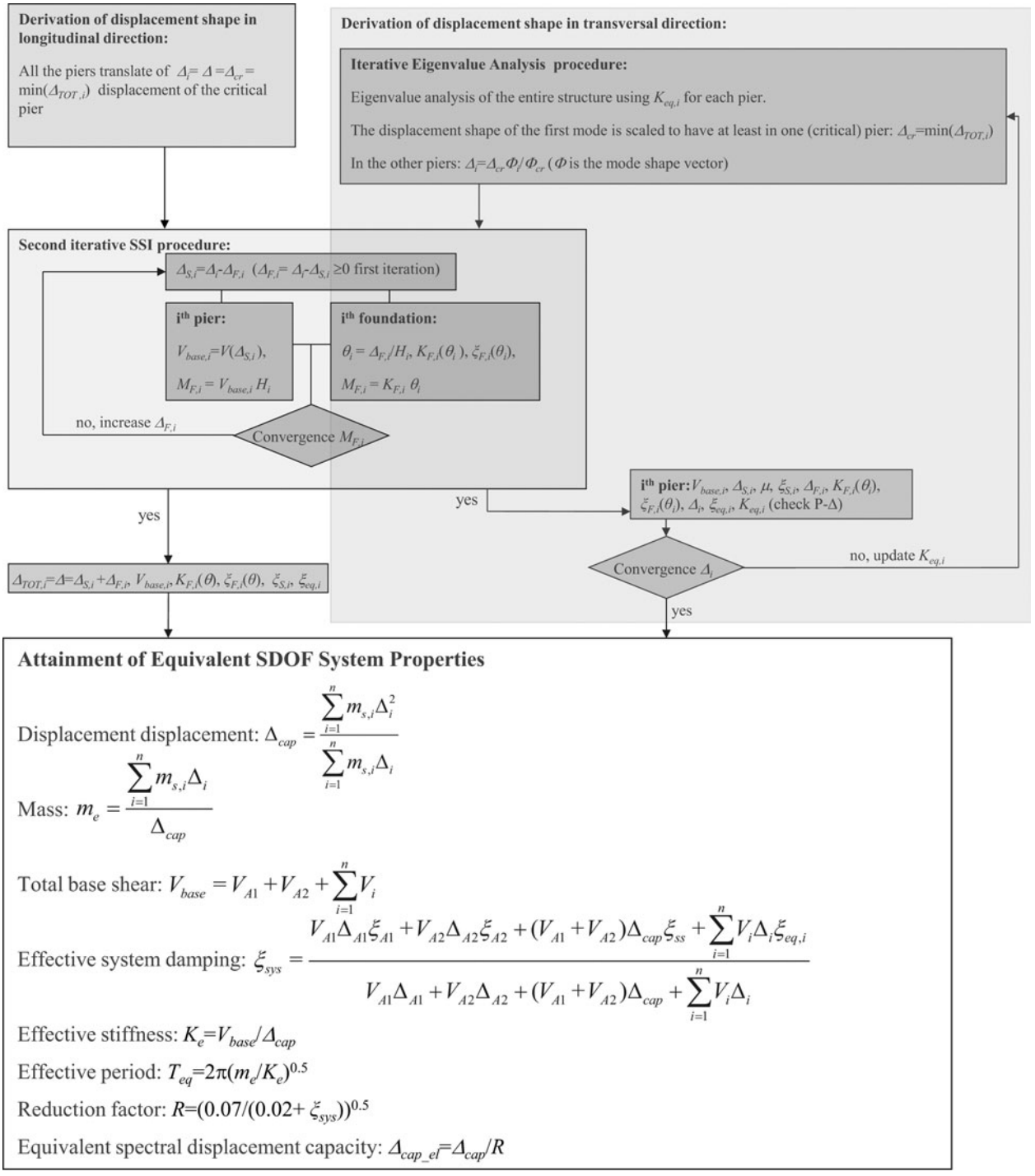

Figure 4. Step 2: reduction of the bridge to a SDOF system.

(OTM_i), is calculated to determine if the P–Δ effect influences the base shear force acting on each pier:

$$\theta_{\Delta,i}=\frac{M_{\mathrm{P}-\Delta,i}}{\mathrm{OTM}_i}=\frac{(m_{\mathrm{S},i}g)\Delta_{\mathrm{S},i}}{H_i V_i}. \tag{7}$$

where g is the standard gravity and $m_{\mathrm{S},i}$ is the mass of the ith pier. If the stability index is >0.1 (Pettinga & Priestley, 2007), a reduced base shear force should be calculated according to (Priestley et al., 2007) the following equations:

$$V_{\mathrm{base},i}=V_i-0.5\frac{M_{\mathrm{P}-\Delta,i}}{H_i}, \tag{8}$$

otherwise

$$V_{\text{base},i} = V_i. \tag{9}$$

(iii) Once the base shear for every pier is known, the moment acting on the foundation due to the shear force of the structure is expressed as

$$M_{\text{F},i} = V_{\text{base},i} H_i. \tag{10}$$

(iv) Foundation rotation θ_i of ith pier is computed from the foundation displacement:

$$\theta_i = \frac{\Delta_{\text{F},i}}{H_i}. \tag{11}$$

Introducing the current value of rotation θ_i into the foundation, secant stiffness degradation and damping increase curves, $K_{\text{F},i}$ and $\xi_{\text{F},i}$, are computed. The moment due to the foundation rotation of all piers can be easily calculated as follows:

$$M_{\text{F},i} = K_{\text{F},i}\theta_i. \tag{12}$$

For each pier, the moments acting on the foundation calculated with Equations (10) and (12) will be compared. If the two values differ by $<1\%$, the convergence is reached. Otherwise, the initial assumed lateral displacement $\Delta_{\text{F},i}$ due to foundation rotation in the beginning of the second iterative NLSSI process will be slightly increased (i.e. 0.0001 m) and will be used as starting value for a new iteration of the process. Once the convergence on the acting moment is obtained, the second iterative NLSSI process is completed.

Typically, the convergence was achieved within five iterations. At the end of the procedure, for the case of seismic action in longitudinal direction, the following quantities are known for the ith pier: total displacement, $\Delta_i = \Delta$; structural displacement, $\Delta_{\text{S},i}$; displacement due to foundation rotation, $\Delta_{\text{F},i}$; base shear, $V_{\text{base},i}$; foundation rotational stiffness, $K_{\text{F},i}$; foundation rotational damping, $\xi_{\text{F},i}$. With respect to step 1, a new value of ductility $\mu = \Delta_{\text{S},i}/\Delta_{\text{Y},i}$ is calculated; thus, according to Equations (1) and (5), the structural damping $\xi_{\text{S},i}$ and the equivalent damping $\xi_{\text{eq},i}$ are updated.

S2.3 Derivation of the bridge displacement shape in transversal direction

In this case, the second NLSSI iterative procedure is nested into IEA which has to be performed (Şadan et al., 2012) to calculate the displacement shape of the bridge a priori unknown. The main purpose of IEA is to compute the displacement pattern of the bridge according to the first mode shape, which means that only the critical pier will experience the maximum possible displacement obtained at the end of the first iterative NLSSI process. Furthermore, the total displacement of the other piers will be scaled down according to the mode shape. Once for each pier and foundation system, the overall maximum possible displacement Δ_i is obtained, the second iterative NLSSI process will be used for calculating the modified pier displacement $\Delta_{\text{S},i}$, base shear $V_{\text{base},i}$, foundation displacement $\Delta_{\text{F},i}$, foundation damping $\xi_{\text{F},i}$ and rotational stiffness $K_{\text{F},i}$, and the system equivalent stiffness ($K_{\text{eq},i} = V_{\text{base},i}/\Delta_i$) will be evaluated correspondingly.

The updated equivalent stiffness of each pier, combined with that of the abutment and deck which are assumed to remain elastic during the seismic action, is used to carry out the next eigenvalue analysis. At the first iteration, the pier stiffness values obtained from the first iterative NLSSI process according to Equation (4) are used for IEA. The iterative procedure will be continued till there is no significant change in the displacement shape of the bridge. IEA normally converges very quickly; however, the inclusion of second iterative NLSSI process may increase the calculation work. When the IEA + -second iterative NLSSI process is finished, the same pier properties already described for the case of longitudinal action are known.

S2.4 Attainment of equivalent SDOF properties

This is the characteristic step of direct displacement-based approaches. The nonlinear multi-degree of freedom system is converted into an SDOF with equivalent linear properties, which are calculated by linearising the system response at the maximum displacement. In the following, the authors briefly recall the formula used for calculating the SDOF properties, while they refer to Şadan et al. (2012) for a detailed description of the procedure.

(i) Displacement capacity Δ_{cap}:

$$\Delta_{\text{cap}} = \frac{\sum_{i=1}^{n} m_i \Delta_i^2}{\sum_{i=1}^{n} m_i \Delta_i}, \tag{13}$$

where m_i and Δ_i, respectively, are the mass and displacement of the ith significant mass location, i.e. at the top of the piers and at the abutment. The abutment mass is assumed equal to half of the weight of the external spans.

(ii) Equivalent mass m_{e}:

$$m_{\text{e}} = \frac{\sum_{i=1}^{n} m_i \Delta_i}{\Delta_{\text{cap}}}. \tag{14}$$

(iii) Total base shear V_{base}:

$$V_{\text{base}} = V_{\text{A1}} + V_{\text{A2}} + \sum_{i=1}^{n} V_{\text{base},i}. \tag{15}$$

V_{A1} and V_{A2} are the base shears acting on the abutments, and since the abutments are assumed to remain elastic during the seismic excitation, they are immediately calculated once the displacements (Δ_{A1} and Δ_{A2}) are known.

(iv) Global system damping ξ_{sys}:

$$\xi_{sys} = \frac{V_{A1}\Delta_{A1}\xi_{A1} + V_{A2}\Delta_{A2}\xi_{A2} + (V_{A1}+V_{A2})\Delta_{cap}\xi_{ss} + \sum_{i=1}^{n} V_{base,i}\Delta_i\xi_{eq,i}}{V_{A1}\Delta_{A1} + V_{A2}\Delta_{A2} + (V_{A1}+V_{A2})\Delta_{cap} + \sum_{i=1}^{n} V_{base,i}\Delta_i}. \quad (16)$$

where ξ_{sys} is calculated using a weighted average based on the energy dissipated by different structural elements. In particular, ξ_{A1} (ξ_{A2}) is the elastic damping of the abutment 1 (2), ξ_{ss} represents the elastic damping assigned to the superstructure and $\xi_{eq,i}$ is the equivalent viscous damping of the ith pier calculated as described in the previous section.

(v) Effective stiffness K_e:

$$K_e = \frac{V_{base}}{\Delta_{cap}}. \quad (17)$$

(vi) Effective period T_e:

$$T_e = 2\pi\sqrt{\frac{m_e}{K_e}}. \quad (18)$$

2.3 *Step 3: assessment of the bridge*

Following Şadan et al. (2012), the assessment of the bridge is performed using a simple pass/fail method based on capacity/demand ratio:

$$\frac{C}{D} = \frac{\Delta_{cap-el}}{\Delta_{dem-el}}. \quad (19)$$

The equivalent elastic displacement demand $\Delta_{dem\text{-}el}$ is figured out from the 5% damped elastic displacement spectrum, selected on the basis of the studied limit state, in accordance to the effective period T_e. The elastic displacement capacity of the equivalent SDOF system $\Delta_{cap\text{-}el}$ is obtained from the previously calculated displacement capacity Δ_{cap} using spectral reduction factor (CEN, 2003) R as derived from the following equations:

$$R = \left[\frac{0.07}{(0.02+\xi_{sys})}\right]^{0.5}, \quad (20)$$

$$\Delta_{cap-el} = \frac{\Delta_{cap}}{R}. \quad (21)$$

For the considered seismic action, the bridge is verified if the ratio C/D is >1 and it will be much less prone to failure, the higher the safety factor is.

3. Application of DDBA + NLSSI procedure to hypothetical bridges

The proposed DDBA + NLSSI procedure was applied to several selected hypothetical cases characterised by straight bridges with deck supported on bearings. Five configurations are considered (Restrepo, 2006) to be obtained from a reference geometry by varying the height of the piers given in H unit. The latter is taken constant as 10 m in this study. The reference geometry (Figure 5) is characterised by six spans; the side span length is 40 m, whereas the middle span length is 50 m. All piers are single column resting on circular shallow foundations and having constant height equal to H. From this geometry, two symmetric configurations were derived with the following pier height sequences: H–1.5H–2H–1.5H–H and 2H–1.5H–H–1.5H–2H. Other two non-symmetric configurations were considered varying the pier height: 2H–1.5H–H–H–1.5H and 2H–H–3H–2H–H.

The piers have a circular section with a diameter of 2 m. A total number of 64 bars with 25 mm diameter, corresponding to an area equal to 1% of the section area, are used as longitudinal reinforcements. The 10-mm-diameter transverse reinforcement is spaced at 10 cm and the cover concrete thickness is 6 cm. All sections have been analysed considering unconfined concrete strength of 40 MPa, confined concrete strength of 42.51 MPa, steel yield stress of 455 MPa and fracture stress of 600 MPa for a fracture strain of 0.12. The Young's modulus for concrete and reinforcement is 30 and 200 GPa, respectively. Concrete material weight is 24 kN/m^3. The deck has a distributed weight of 175 kN/m and a moment of inertia of 44.41 m^4 in both directions. The abutments have effective elastic stiffness of 75,000 kN/m in both directions. Following the simplified assumption of

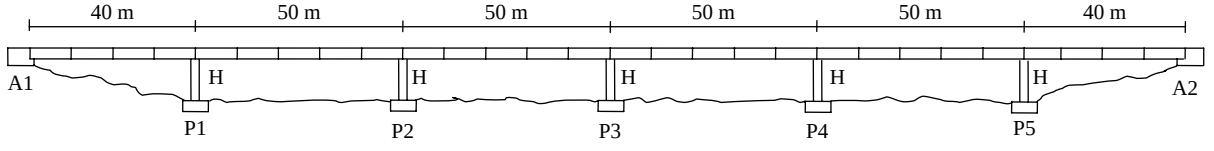

Figure 5. Reference geometry from which five hypothetical bridge configurations, to be studied with DDBA + NLSSI procedure, have been extracted.

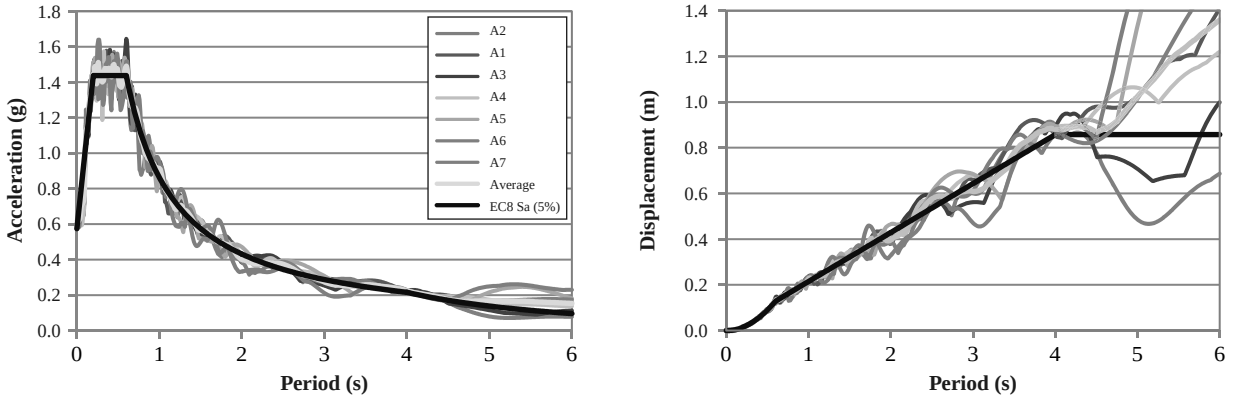

Figure 6. Acceleration and displacement response spectra for the IDA.

disregarding the deformation of the elastomeric bearings, they are described as *simple hinges* (Botero, 2004). Dense sand conditions are chosen for shallow foundations, characterised by friction angle $\varphi = 35°$, shear modulus $G = 72$ MPa, Poisson's ratio $\nu = 0.21$, cohesion $c = 45$ kPa and shear wave velocity at ground surface $V_s = 200$ m/s. The diameter of the circular shallow foundation for 10 and 15 m piers is 7 m, whereas for 20 and 30 m piers is 7.5 m. Constant embedment depth is selected as $h_F = 1.5$ m.

The reliability of the results obtained by the DDBA + -NLSSI procedure was verified by performing incremental dynamic analysis (IDA) (Vamvatsikos & Cornell, 2002). IDA involves performing multiple nonlinear dynamic analyses of a structural model under a suite of ground motion records, which are scaled to several levels of seismic intensity. The selected unscaled accelerograms were compatible with the spectrum adopted in the DDBA + NLSSI procedure. For each intensity level and corresponding scale factor considered, the maximum top displacement of each pier was recorded and compared with its displacement capacity from DDBA + NLSSI analyses. When one of the pier tops reached the displacement capacity, the corresponding scale factor was recorded as capacity/demand ratio to be compared with the obtained DDBA + NLSSI result. Moreover, the same configurations were studied neglecting NLSSI and hence simply using DDBA procedure, with the aim of evaluating the influence of NLSSI in the assessment procedure.

3.1 Analysis background

The described DDBA + NLSSI procedure was implemented in a series of MathCAD subroutines. Moment–curvature and force–displacement responses of the piers were achieved using the cross-sectional analysis program CUMBIA (Montejo & Kowalsky, 2007). The finite-element program SeismoStruct (SeismoSoft, 2010), capable of performing static and dynamic nonlinear analyses of frame structures, was chosen to conduct IDA runs. The material of reinforcing steel and concrete followed the constitutive relationship proposed by Menegotto and Pinto (1973) and Mander, Priestley, and Park (1988), respectively. All pier sections were modelled using the implicit beam-column fibre element with a discretisation of 200 fibres. Elastic beam elements were utilised to represent the deck, while the abutments were modelled as linear elastic spring elements in both directions. The foundation system was modelled using the macro-element developed by Correia (2011), which is capable of taking into account NLSSI effects. For the macro-element parameter calibration and implementation validation, the reader can refer to Ni (2012). A tangent stiffness proportional damping was employed in global stiffness settings.

Although suitable approaches to define displacement-spectrum-compatible real acceleration time histories are in progress (Smerzini, Paolucci, Galasso, & Iervolino, 2012), for simplicity the authors selected seven artificial input accelerograms for IDA generated by the SIMQKE code (Carr, 2007) since their main purpose is the validation of the procedure and they aimed at reducing possible sources of variability of results. The accelerograms are compatible with the Eurocode 8 (EC8) (CEN, 2003) design spectrum Type 1, considering a peak ground acceleration $a_g = 0.5\,g$ on soil type B ($V_{s,30}$ between 360 and 760 m/s). Displacement and acceleration response spectra of each accelerogram were derived utilising SeismoSignal (SeismoSoft, 2011). The mean of the seven spectra is displayed in Figure 6 along with EC8 elastic spectrum for 5% damping level.

3.2 Results for DDBA + NLSSI procedure in longitudinal and transversal directions

The procedure was applied considering both longitudinal and transversal seismic actions for significant damage limit state. The corresponding material strains for concrete and steel were calculated as 0.0071 and 0.072, respectively, according to the formula proposed by

Table 3. Force–displacement responses of the piers of the studied straight bridges with deck supported on bearings.

	Side piers			Mid-piers			
Units (m/kN/ton)	10 m	15 m	20 m	10 m	15 m	20 m	30 m
F_Y	1837.3	1227.46	925.23	1886.37	1262.8	953.63	639.31
F_U	1829.63	1225.86	920.21	1874.4	1249.32	939.84	631.52
Δ_Y	0.084	0.185	0.325	0.084	0.185	0.326	0.723
Δ_U*	0.263	0.545	0.928	0.259	0.536	0.912	1.955

*Significant damage limit state displacement corresponds to the calculated ultimate value.

Priestley et al. (2007). Moment–curvature analysis was performed for each pier when force–displacement bilinearised curve (Table 3) was derived in accordance with plastic hinge concept. The shear strength of all piers was found to be large enough to ensure full flexural response, according to the modified UCSD model (Priestley et al., 1996). In the following step, bridges were transformed into equivalent SDOF systems, and finally, the capacity/demand ratios were determined. The results of the calculations are given in Tables 4 and 5 for the longitudinal and transversal directions, respectively.

IDA was performed for all the selected cases to verify DDBA + NLSSI results with respect to capacity/demand ratios. The use of artificial accelerograms strongly reduced the variability of nonlinear time-history analyses results; however, some dispersion among the results in terms of *C/D* was still present, which was taken into account for the validation of the methodology. For this reason, in the comparison between DDBA + NLSSI and IDA results, both the IDA *C/D* ratio mean value and the range of IDA *C/D* ratio ± standard deviation were considered. The standard deviation σ and coefficient of variation c_v of the

Table 4. Results of the DDBA + NLSSI procedure for the longitudinal response of the studied bridges.

Units (m/kN/ton)	Bridge 1	Bridge 2	Bridge 3	Bridge 4	Bridge 5
Δ	0.371	0.373	0.371	0.371	0.371
ξ_{sys} (%)	6.5	5.9	5.7	5.9	5.7
T_e	1.108	1.133	1.146	1.132	1.153
$\Delta_{cap\text{-}el}$	0.408	0.397	0.389	0.395	0.390
$\Delta_{dem\text{-}el}$	0.237	0.243	0.245	0.243	0.247
C/D	1.721	1.634	1.583	1.629	1.578

Table 5. Results of the DDBA + NLSSI procedure for the transversal response of the studied bridges.

Units (m/kN/ton)	Bridge 1	Bridge 2	Bridge 3	Bridge 4	Bridge 5
M (%)	78.4	78.8	80.8	80.1	78.6
ξ_{sys} (%)	14.1	12.5	11.0	12.0	11.4
T_e	2.32	3.691	2.848	2.626	3.295
$\Delta_{cap\text{-}el}$	0.444	0.944	0.406	0.424	0.490
$\Delta_{dem\text{-}el}$	0.497	0.791	0.61	0.563	0.706
C/D	0.893	1.194	0.666	0.753	0.695

Table 6. Comparison of IDA and DDBA + NLSSI results for the longitudinal response of the studied bridges.

	Method						
	IDA				DDBA + NLSSI		
Bridges	*C/D*	σ	c_v	*C/D* ± σ range	*C/D*	Difference	Error (%)
Bridge 1	1.650	0.139	0.084	1.502 − 1.928	*1.721*	0.071	4.30
Bridge 2	1.679	0.222	0.132	1.461 − 2.035	*1.634*	0.045	2.70
Bridge 3	1.619	0.215	0.133	1.363 − 1.879	*1.583*	0.036	2.24
Bridge 4	1.690	0.175	0.104	1.492 − 1.943	*1.629*	0.061	3.61
Bridge 5	1.535	0.185	0.120	1.276 − 1.794	*1.578*	0.043	2.77
Error level (%)	0–5	5–10	10–15	15–20	>20		

Table 7. Comparison of IDA and DDBA + NLSSI results for the transversal response of the studied bridges.

	Method						
	IDA				DDBA + NLSSI		
Bridges	*C/D*	σ	c_v	*C/D* ± σ range	*C/D*	Difference	Error (%)
Bridge 1	0.893	0.086	0.097	0.759 − 0.993	*0.893*	0.000	0.00
Bridge 2	1.177	0.141	0.120	0.974 − 1.341	*1.194*	0.017	1.47
Bridge 3	0.641	0.089	0.138	0.551 − 0.805	*0.666*	0.025	3.97
Bridge 4	0.798	0.133	0.166	0.647 − 0.985	*0.753*	0.045	5.63
Bridge 5	0.683	0.099	0.144	0.585 − 0.876	*0.695*	0.012	1.69
Error level (%)	0–5	5–10	10–15	15–20	>20		

results were calculated as follows:

$$\sigma = \sum_{i=1}^{n} (x_i - x_m)^2 \quad \text{and} \quad c_v = \frac{\sigma}{x_m}, \tag{22}$$

where x_i is the *C/D* ratio for the *i*th accelerogram and x_m is the mean of the *C/D* ratios of all accelerograms.

In particular, as shown in Tables 6 and 7, where longitudinal and transversal results are summarised, for each studied case, the *C/D* ratio obtained with DDBA + -NLSSI was written in italic if it fit in the range of IDA *C/D* ratio ± σ, if it did not fit it was written in bold, whereas the percentage error between the mean values of *C/D* ratio was calculated and classified with a grey colour scale according to the magnitude. In both longitudinal and transversal cases, DDBA + NLSSI results are consistent with those of IDA since the largest error is <6% and all DDBA + NLSSI *C/D* ratios are within the range of IDA *C/D* ratios ± σ.

All selected bridges have a safety factor with respect to a potential longitudinal seismic risk >1.5 (see Table 6). This is probably due to present limitations of the process, and, in particular, to the fact that only the attainment of the maximum displacement capacity of one of the piers is assumed as possible failure mode for the bridge. Nevertheless, along their longitudinal direction, bridges

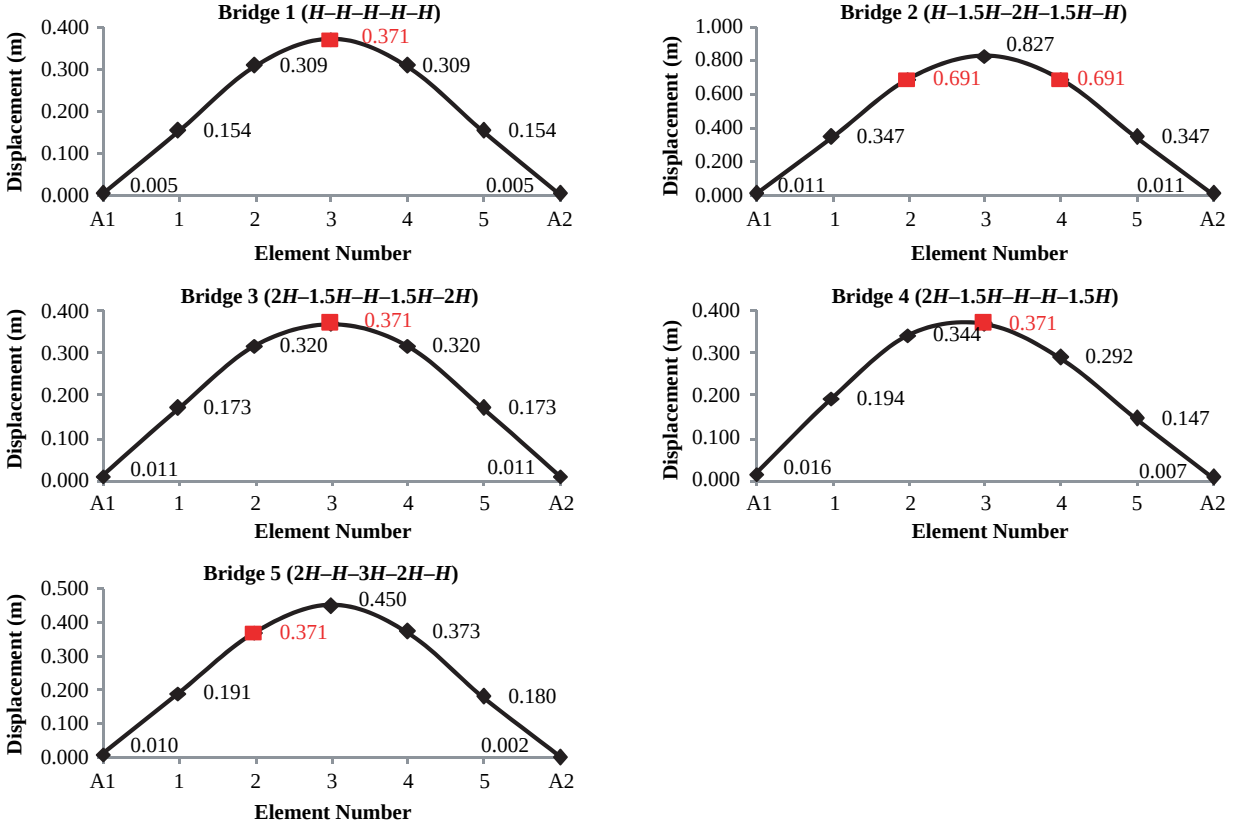

Figure 7. The resultant displacement shapes in transversal direction from DDBA + NLSSI procedure for the studied bridges.

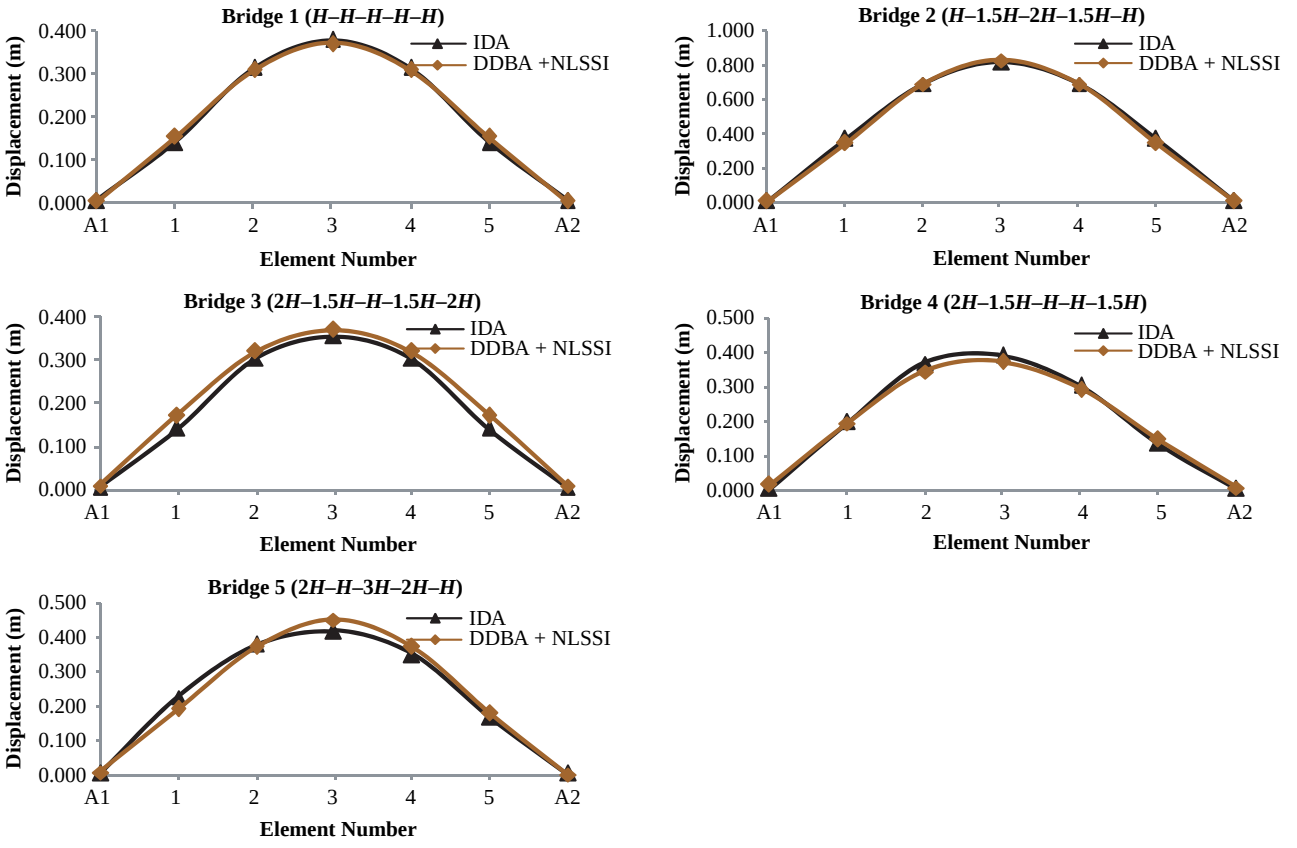

Figure 8. Comparison of resultant displacement shapes in transversal direction between IDA and DDBA + NLSSI procedure for the studied bridges.

are more often subjected to deck or girder failures because of insufficient seating space, bearing failures, absence of shear keys, abutments failure, etc. Further developments for overcoming these limitations are under development. However, at this stage, the aim (that led to the specific simple examples) was not to apply the procedure to a real bridge but to verify that the procedure, under the considered assumptions, gives coherent results.

In the transversal direction, the bridges have worst performance: in four of the five cases, the capacity is lower than the demand, i.e. bridges 1, 3, 4 and 5 are prone to failure for significant damage limit state. This may be attributed to the fact that plastic hinge formation and the following attainment of the maximum displacement capacity of one of the piers is one of the most common reasons of collapse in case of transversal response. There is also a higher variability in the error as well as in the safety factor values (Table 7), which is due to the fact that deriving the displacement shape for the evaluation of the bridge displacement capacity is more complex and is affected by changes in bridge pier heights. The displacement shapes and the critical piers obtained from the application of IEA + second iterative NLSSI process are plotted in Figure 7. It can be easily noticed that, in all the cases, the NLSSI identifies the critical pier as the shortest one among the three central piers: in bridges 1, 3, 4 and 5, the critical pier has height equal to 10 m (H), whereas in bridge 2, it has height equal to 15 m (1.5H). Moreover, NLSSI allows the critical pier to reach a displacement greater than the limit state displacement Δ_{SL} calculated as in sub-step S1.1 and reported in Table 3.

During IDA in transversal direction, once the mean value of capacity/demand ratios is evaluated, it is applied as scale factor to the set of previously used accelerograms, and new nonlinear time-history analyses are performed for each bridge. The mean value of the obtained displacement profile envelopes is used for comparison with the resultant displacement shapes from DDBA + NLSSI analysis (Figure 8). The good agreement between the results is mainly due to the fact that, for all the cases, the dynamic behaviour is dominated by the first mode shape (also the mass participation factor of the first mode in transversal directions is always around 80%, as shown in Table 5); thus, the IEA procedure is able to fit accurately the final displacement shape. Moreover, the prevalence of the first mode implies a higher displacement demand in the central piers. Accordingly, the cases with C/D ratios less than one are those where the pier with height equal to H is in the

Table 8. Comparison of DDBA (fixed-base conditions) and DDBA + NLSSI results for the transversal response of the studied bridges.

	Bridge 1		Bridge 2		Bridge 3		Bridge 4		Bridge 5	
Units (m/kN/ton)	DDBA	DDBA + SSI	DDBA	DDBA + SSI	DDBA	DDBA + SSI	DDBA	DDBA + SSI	DDBA	DDBA + SSI
M (%)	76.2	78.4	78.3	78.8	81.3	80.8	79.5	80.1	77.5	78.6
Δ_{cap}	0.202	0.293	0.507	0.656	0.210	0.299	0.212	0.299	0.247	0.355
m_e	4115	4206	4248	4267	4389	4370	4271	4311	4253	4300
V_{base}	9142	9032	8095	8111	6479	6352	7302	7390	5400	5550
$\xi_{sys(\%)}$	12.2	14.1	12.6	12.5	9.2	11.0	10.6	12.0	9.5	11.4
R_ξ	0.702	0.659	0.693	0.695	0.79	0.735	0.746	0.707	0.78	0.724
K_e	45,360	30,850	14,500	12,370	30,940	21,270	34,400	24,680	20,760	15,640
T_e	1.892	2.32	3.401	3.691	2.367	2.848	2.213	2.626	2.844	3.295
$\Delta_{cap\text{-}el}$	0.287	0.444	0.731	0.944	0.265	0.406	0.284	0.424	0.316	0.490
$\Delta_{dem\text{-}el}$	0.405	0.497	0.729	0.791	0.507	0.61	0.474	0.563	0.609	0.706
C/D	0.708	0.893	1.003	1.194	0.523	0.666	0.599	0.753	0.519	0.695

central zone. In particular, the worst cases correspond to bridges 3 and 5, where higher piers are at the two sides of the critical one ($1.5H–H–1.5H$ and $2H–H–3H$, respectively). This remark highlights the strict relationship between the failure mode due to the attainment of the maximum displacement capacity and bridge geometry.

Finally, for the seismic action in transversal direction, the same bridge configurations were studied using DDBA under the hypothesis of fixed-base piers. Table 8 compares the DDBA and DDBA + NLSSI procedure results. It is interesting to notice that in all the cases, the NLSSI has beneficial effects since it increases the equivalent period of the SDOF system and, accordingly, its capacity as well. The displacement shapes and the critical piers obtained from the application of IEA for DDBA are plotted in Figure 9. It can be observed that in contrast to the case of DDBA + NLSSI, the critical pier is always the shortest pier ($H = 10$ m). From the comparison between IDA and DDBA (Table 9), it results that the maximum error is slightly higher than in the case of DDBA + NLSSI (6.6% vs 5.6%) and it refers to the third bridge, whereas in the case of DDBA + NLSSI, it was found for the fourth bridge. This is a direct indication that taking into account NLSSI effects may also affect the assessment results in terms of selection of the more vulnerable bridge.

4. Conclusions

In this work, the authors have developed a practical, but also sufficiently accurate, seismic assessment procedure for multi-span reinforced concrete bridges, based on DDBA + NLSSI. Although limited in this paper to hypothetical simple bridge configurations, its application to an existing bridge (Ni, 2012), not presented herein for brevity, confirmed the presented satisfactory results.

Nevertheless, several limitations are still present in the procedure: (i) the application is limited to simple straight-bridge configurations, with single-column piers and continuous deck supported on bearings or monolithically connected with the piers without expansion/seismic gaps; (ii) the failure is controlled by the attainment of maximum displacement capacity of one of the piers, whereas other modes of failure, e.g. involving deck, abutment, bearings and soil–foundation, are neglected; (iii) the NLSSI effects are presently limited to the case of shallow foundations on sand, while extension to deep foundations is still in progress; (iv) the influence of higher modes is neglected; (v) base-isolated bridges are not considered. Obviously, as previously discussed, these limitations influence the results of the procedure. In particular, they affect the safety factor and hence all the considered bridge configurations have a safe longitudinal response ($C/D > 1$), whereas they are prone to failure in transversal direction ($C/D < 1$ for all bridges except from bridge 2).

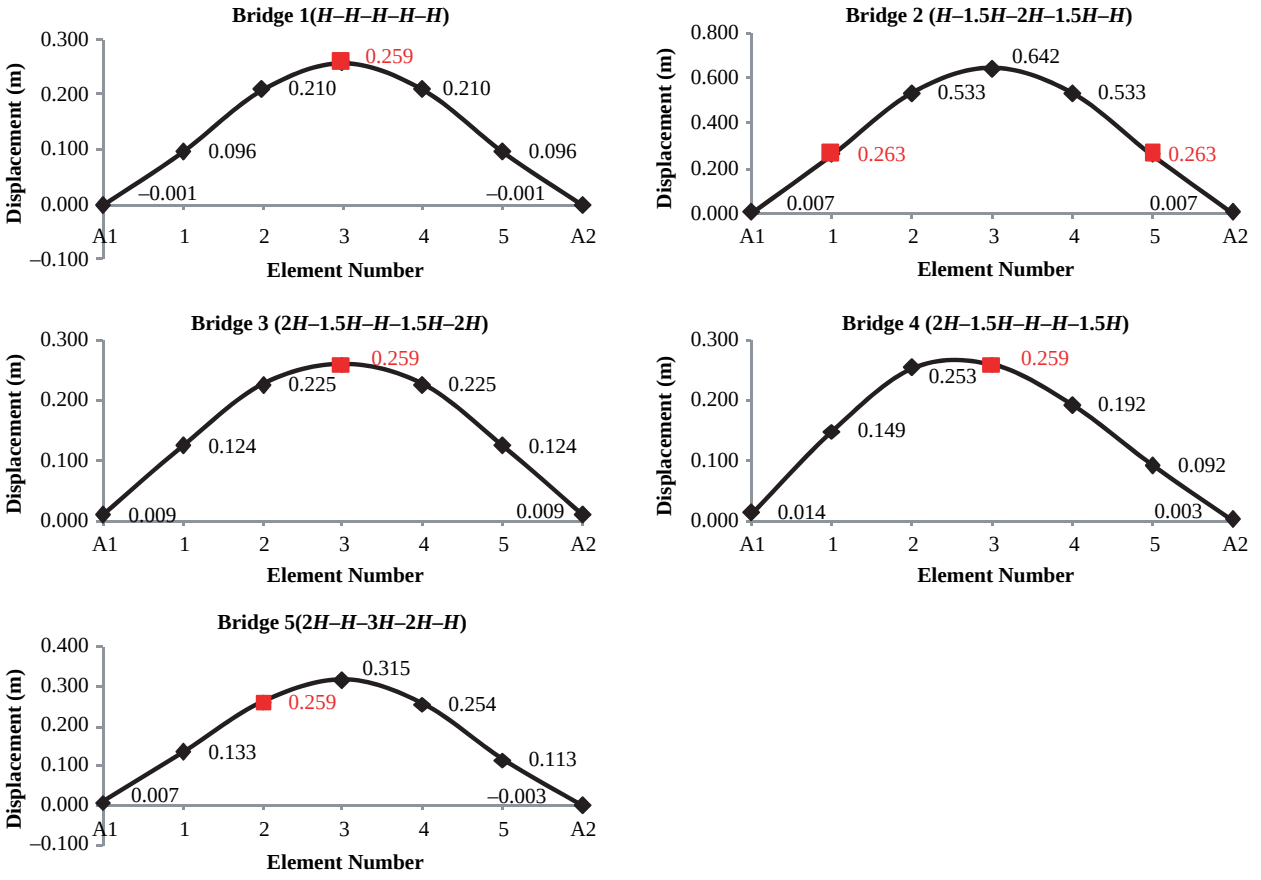

Figure 9. The resultant displacement shapes in transversal direction from DDBA procedure for the studied bridges with fixed base conditions.

Table 9. Comparison of IDA and DDBA results for the transversal response of the studied bridges.

	Method				
	IDA		DDBA		
Bridges	*C/D*	*C/D* range	*C/D*	Difference	Error (%)
Bridge 1	0.692	0.559–0.792	*0.708*	0.016	2.31
Bridge 2	0.966	0.846–1.146	*1.003*	0.037	3.79
Bridge 3	0.491	0.401 – 0.655	*0.523*	0.032	6.62
Bridge 4	0.589	0.412–0.735	*0.599*	0.010	1.68
Bridge 5	0.497	0.430–0.573	*0.519*	0.022	4.32
Error level (%)	0–5	5–10	10–15	15–20	>20

Moreover, although NLSSI was found to have beneficial effects in all the cases as it has led to reduction in pier ductility demand, on the other hand, it has also increased the total displacement with potential harmful effects for the deck or the connection between pier and deck.

However, owing to the initial stage of this research, preference is given to keep the procedure as simple as possible to highlight its main steps and to validate it without introducing too many sources of uncertainty. Furthermore, while part of the previous limitations can be overcome without undermining the need of simplicity, it is believed that the main field of application of the proposed procedure should be the first-level screening of existing bridges with potentially important NLSSI effects. Hence, it can be utilised as an efficient tool for a quick and adequately accurate assessment of existing bridges in order to prioritise maintenance actions. After the selection of structures at risk, a second and more accurate assessment should be performed accounting for structural, foundation and interaction modelling in a more elaborate manner to capture their true dynamic nonlinear response. Finally, it is noted that the simplicity of the procedure

supports its application in the framework of probabilistic performance-based approaches to risk assessment, allowing bridge engineers to perform fast parametric analyses for calibration of fragility curves.

Acknowledgements

This work was partially funded by the Italian Department of Civil Protection and by the Rete dei Laboratori Universitari di Ingegneria Sismica (ReLUIS), in the framework of the DPC-RELUIS Research Programme (2010–2013), Line 2, 'Displacement-based vulnerability assessment'. The authors also gratefully acknowledge the funding supports from the Category A Scholarship, which is directly sponsored by the European Commission, under the scope of its Erasmus Mundus programme – Master in Earthquake Engineering and Engineering Seismology (MEEES).

References

Botero, J.C.A. (2004). *Displacement-based design of continuous concrete bridges under transverse seismic excitation* (Master's dissertation). European School for Advanced Studies in Reduction of Seismic Risk (ROSE School), Pavia, Italy.

Cardone, D., Perrone, G., & Sofia, S. (2011). A performance-based adaptive methodology for the seismic evaluation of multi-span simply supported deck bridges. *Bulletin of Earthquake Engineering*, *9*(5), 1463–1498.

Carr, A.J. (2007). *SIMQKE: A program for artificial motion generation*. Christchurch: Civil Engineering Department, University of Canterbury.

CEN (2003). *Eurocode 8, Design of structures for earthquake resistance. Part 1: General rules, seismic actions and rules for buildings, prEN 1998-1, draft no. 6*. Brussels: Comité Européen de Normalisation.

Correia, A.A. (2011). *A pile-head macro-element approach to seismic design of monoshaft-supported bridges*, (Doctoral dissertation). European School for Advanced Studies in Reduction of Seismic Risk (ROSE School), Pavia, Italy.

Deng, L., Kutter, B.L., & Kunnath, S. (2012). Centrifuge modeling of bridge systems designed for rocking foundations. *ASCE Journal of Geotechnical and Geoenvironmental Engineering*, *138*(3), 335–344.

Drosos, V., Georgarakos, T., Loli, M., Anastasopoulos, I., Zarzouras, O., & Gazetas, G. (2012). Soil–foundation–structure interaction with mobilization of bearing capacity: An experimental study on sand. *ASCE Journal of Geotechnical and Geoenvironmental Engineering*, *138*(11), 1369–1386.

Dwairi, H., & Kowalsky, M.J. (2006). Implementation of inelastic displacement patterns in direct displacement based design of continuous bridge structures. *Earthquake Spectra*, *22*(3), 631–662.

Gazetas, G. (1991). Foundation vibration, Chapter 15. In H.-Y. Fang (Ed.), *Foundation engineering handbook* (2nd ed., pp. 553–593). New York: Van Nostrand, Reinhold.

Ghalibafian, H., Foschi, R.O., & Ventura, C.E. (2008). Performance-based assessment of the effects of soil–structure interaction on the seismic demands of bridge piers: A proposed methodology. *14th world conference on Earthquake Engineering*, Beijing, China.

Grant, D.N., Blandon, C.A., & Priestley, M.J.N. (2005). *Modelling inelastic response in direct displacement-based design* (ROSE Research Report 2005/03) Pavia, Italy: IUSS Press.

Kappos, A.J., Gidaris, I.G., & Gkatzogias, K.I. (2012). Problems associated with direct displacement-based design of concrete bridges with single-column piers, and some suggested improvements. *Bulletin of Earthquake Engineering*, *10*(4), 1237–1266.

Kausel, E. (2010). Early history of soil–structure interaction. *Soil Dynamics and Earthquake Engineering*, *30*, 822–832.

Kowalsky, M.J. (2002). A displacement-based approach for the seismic design of continuous concrete bridges. *Earthquake Engineering and Structural Dynamics*, *31*(3), 719–747.

Kwon, O.S., & Elnashai, A.S. (2010). Fragility analysis of a highway over-crossing bridge with consideration of soil-structure interaction. *Structure and Infrastructure Engineering*, *6*(1–2), 159–178.

Liu, W., Hutchinson, T.C., Kutter, B.L., Hakhamaneshi, M., Aschheim, M., & Kunnath, S. (2012). Demonstration of compatible yielding between soil–foundation and superstructure components. *ASCE Journal of Structural Engineering*. Retrieved from http://dx.doi.org/10.1061/(ASCE)ST.1943-541X.0000637

Mander, J.B., Priestley, M.J.N., & Park, R. (1988). Theoretical stress-strain model for confined concrete. *ASCE Journal of Structural Engineering*, *114*(8), 1804–1826.

Menegotto, M., & Pinto, P.E. (1973). Method of analysis for cyclically loaded R.C. plane frames including changes in geometry and non-elastic behaviour of elements under combined normal force and bending. *Symposium on the Resistance and Ultimate Deformability of Structures Acted on by Well Defined Repeats Loads*, Zurich, Switzerland.

Montejo, L.A., & Kowalsky, M.J. (2007). *CUMBIA: Set of codes for the analysis of reinforced concrete members*. (Technical Report No. IS-07-01). Raleigh, NC: Department of Civil, Construction and Environmental Engineering, North Carolina State University.

Mylonakis, G., & Gazetas, G. (2000). Seismic soil structure interaction: Beneficial or detrimental? *Journal of Earthquake Engineering*, *4*(3), 277–301.

Mylonakis, G., Syngros, C., Gazetas, G., & Tazoh, T. (2006). The role of soil in the collapse of 18 piers of Hanshin Expressway in the Kobe earthquake. *Earthquake Engineering and Structural Dynamics*, *35*(5), 547–575.

Ni, P. (2012). *Non-linear dynamic soil–structure interaction for displacement-based seismic assessment of bridges*, (Master's dissertation). European School for Advanced Studies in Reduction of Seismic Risk (ROSE School), Pavia, Italy.

Paolucci, R., di Prisco, C., Figini, R., Petrini, L., & Vecchiotti, M. (2009). Interazione dinamica non lineare terreno-struttura nell'ambito della progettazione sismica agli spostamenti. *Progettazione Sismica*, *2*, 83–103, (in Italian).

Paolucci, R., Figini, R., & Petrini, L. (2013). Introducing dynamic non-linear soil–foundation–structure interaction effects in displacement-based seismic design. *Earthquake Spectra*, *29*(2), 1–22.

Pecker, A., Paolucci, R., Chatzigogos, C., Correia, A., & Figini, R. (2012). The role of non-linear dynamic soil–foundation interaction on the seismic response of structures. *Keynote*

lecture. *2nd international conference on Performance-based Design in Earthquake Geotechnical Engineering*, Taormina, Italy.

Petrini, L., Şadan, O.B., & Calvi, G.M. (2009). Direct displacement-based seismic assessment procedure for multi-span reinforced concrete bridges. *13th Italian conference on Earthquake Engineering*, Bologna, Italy.

Pettinga, J.D., & Priestley, M.J.N. (2007). *Accounting for P–Δ effects in structures when using direct displacement-based design* (ROSE Research Report 2007/02). Pavia, Italy: IUSS Press.

Priestley, M.J.N. (1997). Displacement-based seismic assessment of reinforced concrete buildings. *Journal of Earthquake Engineering*, *1*(1), 157–192.

Priestley, M.J.N., Calvi, G.M., & Kowalsky, M.J. (2007). *Displacement-based seismic design of structures*. Pavia, Italy: IUSS Press.

Priestley, M.J.N., Seible, F., & Calvi, G.M. (1996). *Seismic design and retrofit of bridges*. New York, NY: Wiley.

Restrepo, J.C.O. (2006). *Displacement-based design of continuous concrete bridges under transverse seismic excitation*, (Master's dissertation). European School for Advanced Studies in Reduction of Seismic Risk (ROSE School), Pavia, Italy.

Şadan, O.B. (2009). *Direct displacement-based seismic assessment procedure for multi-span reinforced concrete bridges*, (Doctoral dissertation). Politecnico di Milano, Italy.

Şadan, O.B., Petrini, L., & Calvi, G.M. (2012). Direct displacement-based seismic assessment procedure for multi-span reinforced concrete bridges with single-column piers. *Earthquake Engineering and Structural Dynamics*. doi:10.1002/eqe.2257

SeismoSoft (2010). *SeismoStruct: A computer program for static and dynamic nonlinear analysis of framed structures*, [online]. Retrieved from http://www.seismosoft.com

SeismoSoft (2011). *SeismoSignal: A computer program for signal processing of strong motion data*, [online]. Retrieved from http://www.seismosoft.com

Sextos, A., Kappos, A.J., & Pitilakis, D. (2003). Inelastic dynamic analysis of RC bridges accounting for spatial variability of ground motion, site effects and soil–structure interaction phenomena. Part 2: Parametric study. *Earthquake Engineering and Structural Dynamics*, *32*(4), 629–652.

Sextos, A., Pitilakis, D., & Kappos, A.J. (2003). Inelastic dynamic analysis of RC bridges accounting for spatial variability of ground motion, site effects and soil–structure interaction phenomena. Part 1: Methodology and analytical tools. *Earthquake Engineering and Structural Dynamics*, *32* (4), 607–627.

Smerzini, C., Paolucci, R., Galasso, C., & Iervolino, I. (2012). Engineering ground motion selection based on displacement-spectrum compatibility. *15th world conference on Earthquake Engineering*, Lisbon, Portugal.

Suarez, V.A., & Kowalsky, M.J. (2011). A stability-based target displacement for direct displacement-based design of bridge piers. *Journal of Earthquake Engineering*, *15*(5), 754–774.

Vamvatsikos, D., & Cornell, C.A. (2002). Incremental dynamic analysis. *Earthquake Engineering and Structural Dynamics*, *31*(3), 491–514.

Wolf, J.P. (1985). *Dynamic soil–structure interaction*. Englewood Cliffs, NJ: Prentice Hall.